Organic Chemistry Frontiers (2023): 11st October

DOI: https://doi.org/10.1039/D3QO01471A

View Article Online
DOI: 10.1039/D3QO01471A

ARTICLE

Intramolecular Hydrogen Bond Activation for Kinetic Resolution of Furanone Derivatives by an Organocatalyzed [3+2] Asymmetric Cycloaddition

Received 00th January 20xx,
Accepted 00th January 20xx

DOI: 10.1039/x0xx00000x

Miguel A. Valle-Amores,[a] Claudia Feberero,[a,b] Ana Martín-Somer,[c] Sergio Díaz-Tendero,[d,e,f] Andrew D. Smith,[g] Alberto Fraile*[a,e] and José Alemán*[a,e]

Herein, a formal highly enantioselective organocatalyzed [3+2] cycloaddition of furanone derivatives and azomethine ylides is presented. The success of this reaction resides in an intramolecular hydrogen bond activation through an *o*-hydroxy group at aromatic ring of the imine, allowing the formation of highly multifunctional bicyclic adducts with five stereogenic centers in a stereocontrolled manner. Furthermore, the reaction is paired to a highly efficient kinetic resolution of butenolides, achieving selectivity factors above 200. Using this methodology, furan-2(5*H*)-ones as well as furo[3,4-*c*]pyrrolidinones were obtained with high enantioselectivities. Quantum chemistry calculations reveal the crucial role of hydrogen bond formed between the catalyst donor-units and the two reagents, which modify their arrangement and promote effective facial discrimination resulting in a highly selective kinetic resolution. In addition, further applicability of the kinetic resolution process is shown.

Introduction

The synthesis of chiral compounds in an efficient way has been and still is one of the principal issues within the organic community in both industrial and academic point of view. Among the numerous methods that exist so far, kinetic resolution (KR) is one of the most powerful tools used since it allows, in a very efficient way, the separation of both enantiomers from racemic mixtures.[1]

Regarding the different processes of kinetic resolution, we can distinguish between the use of chiral auxiliaries[1c,2] or catalysts.[1c,3] The principle of KR relies on the reaction of a chiral reagent or catalyst with each enantiomer of the racemic mixture that proceeds through the generation of two diastereomeric transition states. The difference in the free energy between these transition states ($\Delta\Delta G^{\ddagger}$) dictates the difference in rate constants (*k*) for the reaction of each enantiomer, allowing their discrimination and determining the efficiency of the KR by the selectivity factor (*s*) values.[4] The catalytic KR can be divided into enzymatic,[5] which has long been a popular strategy, and non-enzymatic processes,[6] which includes both metal-catalysis[7] and organocatalysis.[8]

Within the plethora of reactions studied for the catalytic kinetic resolution of racemates, [3+2] cycloadditions have been scarcely studied. The first example was described by Fu´s group in 2005, who carried out the kinetic resolution of azomethine imines with activated alkynes catalysed by a chiral copper complex, achieving high enantioselectivities of the recovered dipole and with selectivity factors from 15 to 96 (Scheme 1a).[9] Subsequently, other authors have published metal-catalyzed [3+2] kinetic resolution processes of different racemic dipolarophiles, reaching high *ee* and *s* values.[10] Regarding organocatalyzed [3+2] cycloadditions, up to date, there are only two precedents. The first was reported by Xie´s group in 2010, who carried out the [3+2] cycloaddition of azomethine ylides to nitroolefins catalyzed by Takemoto´s organocatalyst. While this procedure provided the KR of racemic 2-nitro-2*H*-chromene derivatives, the enantioselectivities obtained were from low to moderate (top-Scheme 1b).[11] The second example relates to the three-multicomponent kinetic resolution catalysed by chiral bisphosphoric acids between racemic 2,3-allenoates and *in situ* formed azomethine ylides. In this case, 3-methylenepyrrolidine derivatives were obtained with high enantioselectivities (up to 94% *ee*) with the (*R*)-2,3-allenoates recovered in excellent enantioselectivities (up to 99% *ee*) (bottom-Scheme 1b).[12] It should be noted that, in both antecedents, the authors must make use of azomethine ylides precursors that bears two electron-withdrawing (two esters are present) groups in the

[a] Organic Chemistry Department (Módulo 1), Facultad de Ciencias, Universidad Autónoma de Madrid, 28049-Madrid, Spain. Webpage: www.uam.es/jose.aleman.
[b] Organic Chemistry Area, Chemistry Department, Universidad de Burgos. Burgos-09001, Spain.
[c] Applied Physical Chemistry Department (Módulo 14), Facultad de Ciencias, Universidad Autónoma de Madrid, 28049-Madrid, Spain.
[d] Chemistry Department (Módulo 13), Facultad de Ciencias, Universidad Autónoma de Madrid, 28049-Madrid, Spain.
[e] Institute for Advanced Research in Chemical Sciences (IAdChem), Universidad Autónoma de Madrid, 28049 Madrid, Spain.
[f] Condensed Matter Physics Center (IFIMAC), Universidad Autónoma de Madrid, 28049 Madrid, Spain.
[g] EaStCHEM, School of Chemistry, University of St Andrews, North Haugh, Fife, Scotland, KY16 9ST, UK.

† Dedicate to M. Rosario Martín Ramos for her great contributions on the 5-alcoxyfuran-2(5*H*)-ones chemistry.

Electronic Supplementary Information (ESI) available: [details of any supplementary information available should be included here]. See DOI: 10.1039/x0xx00000x

View Article Online
DOI: 10.1039/D3QO01471A

methylene carbon of imine which, inevitably, limits the structure of the final products.

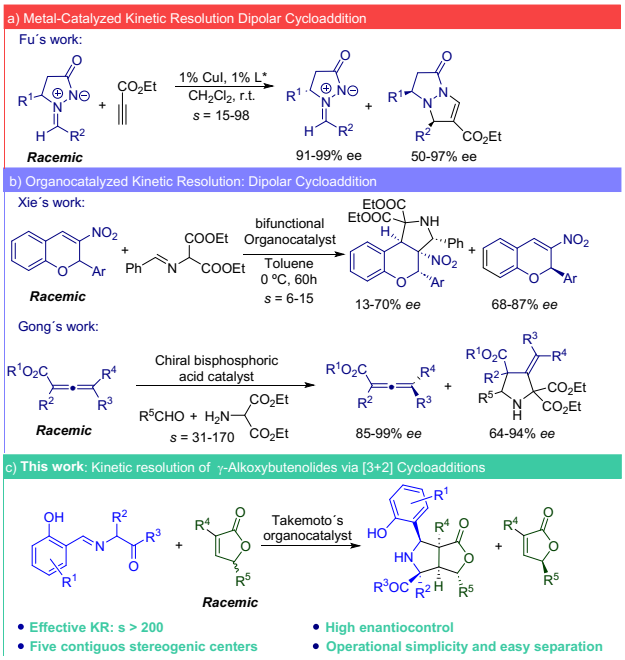

Scheme 1. Catalyzed kinetic resolutions by dipolar cycloaddition reactions.

On the other hand, furanones, a five-membered ring containing an oxygen atom, are a class of heterocyclic compounds of widespread interest in the organic, pharmacology and biological fields, including diverse biological properties such as analgesic, anti-inflammatory, and anticancer among others.[13]

One of the most used synthons that present the butenolide structure are the 5-alkoxyfuran-2(5*H*)-ones which allow to achieve new approaches to acyclic and heterocyclic products.[14-15] Feringa[14c,16] and others[15,17,18] have used butenolide derivatives with chiral auxiliaries such as menthol or sulfinyl groups to achieve diastereoselective asymmetric processes. Starting from these chiral precursors, many interesting structures with high diastereoselectivities have been synthesized. While demonstrative, green chemistry principles consider the use of chiral auxiliaries as not efficient or atom economic, emphasizing the need to develop effective catalyst processes.[19] Therefore, the development of new catalytic procedures to carry out asymmetric reactions with 5-alkoxyfuran-2(5*H*)-ones would be highly desirable. Taking into account the scarce number of examples of organocatalyzed [3+2] kinetic resolutions and the high synthetic value of furan-2(5*H*)-ones, we hypothesized an efficient kinetic resolution could be achieved following a match/mismatch[20] process using a bifunctional organocatalyst and an intramolecular hydrogen bond activation (Scheme 1c).[21]

Results and discussion

Initially, to determine the influence of the hydroxyl group at the imine, we carried out the cycloaddition of the 5-methoxy-2(5*H*)-furanone (**(±)-2a**) with imines **1a** (R= H) and **1b** (R= OH) in the presence of 20 mol% of Takemoto´s catalyst **3a**, obtaining better conversion and enantioselectivity with imine **1b** (Scheme 2). In addition, the reaction with imine **1a** led to a mixture of diasteroisomers (3:1) while with **1b** only one diastereoisomer **4b** was achieved. These results bring to light the important role of the hydroxyl group at the imine on the reactivity and stereoselectivity of this asymmetric process.[21b-c,22] Furthermore, it is remarkable that the selectivity factor (*s*) and the conversion (c) are very high, highlighting the effectiveness of the kinetic resolution of **(±)-2a** (see Table 1, entry 1).

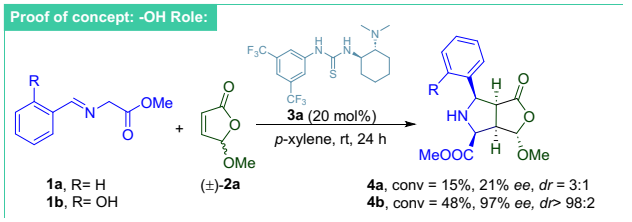

Scheme 2. Proof of concept for the intramolecular H-bond activation: OH role. The reactions were run from 0.1 mmol of imine **1** and 0.1 mmol of **(±)-2a** in 0.3 mL of *p*-xylene ([0.33]M).

Having determined that using imine **1b** affords high selectivity, we continued looking for the optimal reaction conditions. Thus, different bifunctional organocatalyst (20 mol%) were studied, with Takemoto´s thiourea catalyst **3a** giving highest selectivity for this cycloaddition reaction (compare entry 1 with entries 3-8, Table 1). Notably, a racemic background reaction was not operative, as no conversion to product was obtained in the absence of catalyst **3a** (entry 2). The use of squaramide-based catalysts provoked a dramatic loss in conversion (entries 4 and 8). Interestingly, the *pseudo*-enantiomer catalyst **3e** gave very low conversion in comparison with the organocatalyst **3b**. Having identified the most promising catalyst, different solvents were screened (entries 9-12). The use of dichloromethane and *tert*-butylmethylether (entries 9 and 11, respectively) afforded reduced product conversions and enantioselectivities, and hence lower selectivity factors (*s*) than with *p*-xylene (entry 1). However, the reaction in diethylether and toluene (entries 10 and 12) gave rise to good conversion and enantioselectivity, but reduced *s*. Considering the data obtained, *p*-xylene was selected as the best solvent to continue the reaction screening. Subsequently, reaction concentration was also tested, with highest selectivity at [0.33]M, (entry 1) instead of [0.16]M (entry 13) (see SI). Finally, the catalyst loading was studied, with reduced product conversions and selectivity factors (*s*) observed using 15 and 10 mol% catalyst (entries 14 and 15). The reaction was also scaled up to 1.0 mmol, with no detrimental effect on the stereoselectivity and obtaining best results in both, enantiomerical excess and selectivity factor (**4b**: 47% and **2a:** 46% yield, entry 16). Additionally, to determine if the use a lower amount of imine **1b** could provide similar results to the obtained in entry 1, we carried out the reaction starting from

View Article Online
DOI: 10.1039/D3QO01471A

0.05 mmol of **1b** (entry 17). However, the results obtained were worse, achieving only a 68% of enantiomeric excess for furanone (–)-**2a** and lower selectivity factor for the kinetic resolution.

Table 1. Screening reaction conditions.[a]

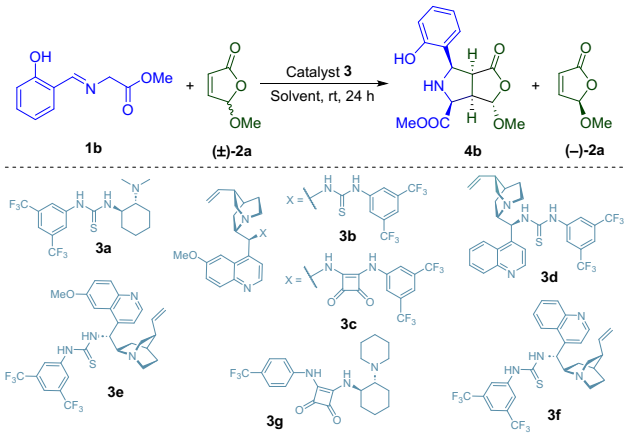

Entry	Cat (mol%)	Solvent	Conv (%)[b]	*ee* **4b** (%)[c]	*ee* **(–)-2a** (%)[c]	*s* (c(%))[d]
1	**3a (20)**	***p*-xylene**	**48**	**97**	**87**	**190 (47)**
2	---	*p*-xylene	<5	---	---	---
3	**3b** (20)	*p*-xylene	40	96	65	100 (40)
4	**3c** (20)	*p*-xylene	10	---	---	---
5	**3d** (20)	*p*-xylene	20	---	---	---
6	**3e** (20)	*p*-xylene	18	---	---	---
7	**3f** (20)	*p*-xylene	19	---	---	---
8	**3g** (20)	*p*-xylene	<5	---	---	---
9	**3a** (20)	CH_2Cl_2	34	86	50	22 (37)
10	**3a** (20)	Et_2O	47	95	91	120 (49)
11	**3a** (20)	MTBE	45	91	82	50 (47)
12	**3a** (20)	Toluene	48	92	98	110 (51)
13[e]	**3a** (20)	*p*-xylene	45	95	81	100 (46)
14	**3a** (15)	*p*-xylene	42	97	76	150 (44)
15	**3a** (10)	*p*-xylene	38	97	55	110 (36)
16[f]	**3a** (20)	*p*-xylene	48	97	92	>200 (49)
17[g]	**3a** (20)	*p*-xylene	40	95	68	80 (41)

[a] The reaction was run from 0.1 mmol of imine **1b** and 0.1 mmol of **(±)-2a** in 0.3 mL of indicated solvent ([0.33]M). [b] Conversion determined by ^{1}H-NMR. [c] Determined by chiral SFC. [d] Calculated conversion (c)=$ee_{SM}/(ee_{SM}+ee_{PR})$, Selectivity factor (*s*)=ln[(1-c)(1-*ee*SM)]/ln[(1-c)(1+*ee*SM)]. [e] [0.16]M instead of [0.33]M. [f] The reaction was scaled up to 1.0 mmol of imine **1b**. [g] The reaction was carried out from 0.05 mmol of imine **1b**.

With the optimized conditions in hand (c = 47%, *s* = 190, Table 1, entry 1), the scope of the dipolar cycloaddition and the efficiency of the KR for **(±)-2a** were evaluated (Scheme 3). For this purpose, a large assortment of imines **1** bearing an *ortho*-hydroxyl group at the aromatic ring and with different substituents were tested. When electron-donating groups are present at the aromatic ring of the imine such as methyl (**1c** and **1d**) or methoxy (**1e** and **1f**) group, cycloaddition products **4c-f** were obtained with high conversions and excellent enantioselectivities (94-99% *ee´s*). Moreover, the (*R*)-5-methoxyfuran-2(5*H*)-one (**(–)-2a**) could be recovered with high yields and good enantioselectivities (86-90% *ee's*), achieving excellent selectivity factor (*s* > 200) for **1c-e**, while for **1f** a reduced but still significant value was obtained (*s* = 90). The presence of an electron-donating diethylamino group (**1g**), maintained the enantioselectivity of the cycloaddition (98% *ee*, s = 170) but led to decreased conversion (c = 25%). Furthermore, halogens at *para*- (**1h-i**) and *meta*-positions (**1j**) were employed. Cycloaddition products **4h-j** were obtained with good conversions and high enantioselectivities (up to 95% *ee* for **4i**). Regrettably, enantioselectivities of the recovered starting materials **(–)-2a** were from moderate to good (up to 87% *ee*), affording reasonable selectivity factors (*s* = 28-80) for the resolution of **(±)-2a**. When a nitro group is present at *meta* position (**1k**), the cycloadduct **4k** and the furanone **(–)-2a** were obtained with excellent enantiomeric excess (95 and 90% *ee*, respectively) and, more important, the conversion (c = 49%) and the selectivity factor (*s* = 120) were very high. An ester group at the *meta* position (**1l**) afforded the cycloaddition product **4l** with good enantioselectivity (91% *ee*), but with decreased conversion and selectivity factor (c = 38%, *s* = 37). Two iminoesters with a naphthyl group (**1m** and **1n**) were reacted at room temperature with the dipolarophile **(±)-2a** under the standard reaction condition without obtaining the corresponding cycloadducts. To our delight, this limitation could be overcome by increasing the temperature to 50 ºC, achieving thus **4m** and **4n** with excellent enantioselectivity values (93 and 97% *ee*, respectively) and with high selectivity factor for both reactions (*s* = 90). Notably, alpha-substituted imines **1o** and **1p**, with a methyl or a phenyl group, respectively, worked well and allowed the asymmetric synthesis of 4-substituted pyrrolidines **4o** and **4p**, bearing a quaternary stereocentre, with good enantioselectivities (87 and 71% *ee*, respectively), high or complete diastereoselectivity (for **4p**: 5:1 *dr*) and elevate conversion (up to 51%). Nevertheless, regarding on the selectivity, the resolution was more effective with the α-, methyl imine (**1o**) (*s* = 45) than with α-phenyl,ring **1p** (*s* = 11). Different electron withdrawing groups at the imine moiety, such as *N,N*-dimethyl amide **1q**, ethyl ester **1r**, and Weinreb´s amide **1s** also lead to corresponding bicyclic adducts **4q-s** in good to high enantioselectivities (84-93% *ee*) and high conversions. The best results in terms of selectivity factor were achieved from Weinreb´s amide **1s** (*s* = 100), which allowed recovery of the (*R*)-5-methoxyfuran-2(*5H*)-one (**(–)-2a**) with excellent enantioselectivity (99% *ee*). The absolute configuration of the stereogenic centres of cycloadduct hydroxylated **4** was assigned by X-ray crystallographic analysis of a monocrystal of **4j** (3*S*,3a*R*,4*S*,6*R*,6a*S*)[23] (middle, Scheme 3) and assuming the same stereochemical outcome for the rest of products.

Finally, to demonstrate the versatility of our [3+2] cycloaddition kinetic resolution, we studied the influence of the incorporation of a variety of substituents at C(3) and C(5) within the furan-2(5*H*)-one as well as the use of 2-(5*H*)-pyrrolones (Scheme 4). Varying substitution at C(5) from methoxy to ethoxy group gave excellent conversion to product, giving an *s* factor >200 for the kinetic resolution and provided resolved (*R*)-

View Article Online
DOI: 10.1039/D3QO01471A

5-ethoxyfuran-2(*5H*)-one (**(–)-2b**) in excellent enantiomeric excess.

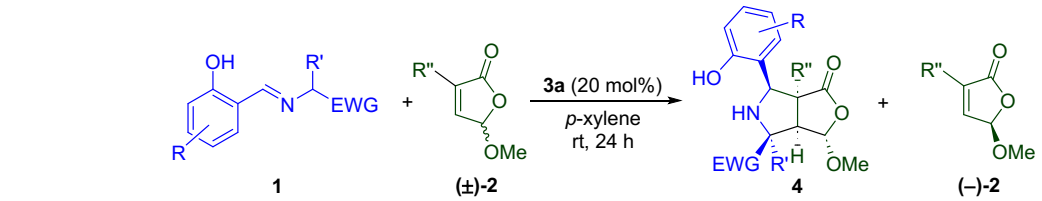

Aromatic substitution at aldimine

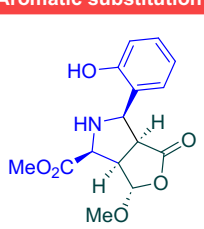

c = 47%; *s* = 190
4b: 97% *ee*; 47%
(–)-2a: 87% *ee*; 43%

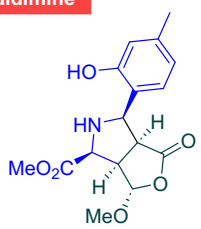

c = 48%; *s* = >200
4c: 99% *ee*; 42%
(–)-2a: 90% *ee*; 41%

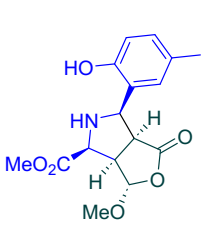

c = 47%; *s* = >200
4d: 98% *ee*; 48%
(–)-2a: 86% *ee*; 41%

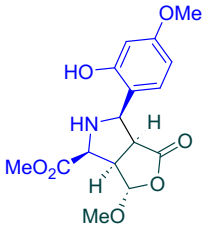

c = 48%; *s* = >200
4e: 97% *ee*; 47%
(–)-2a: 90% *ee*; 45%

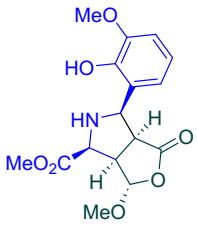

c = 48%; *s* = 90
4f: 94% *ee*; 48%
(–)-2a: 86% *ee*; 44%

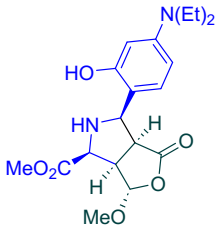

c = 25%; *s* = 170
4g: 98% *ee*; 30%
(–)-2a: 34% *ee*; 60%

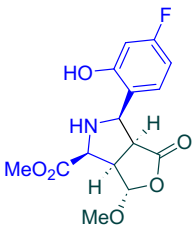

c = 51%; *s* = 28
4h: 82% *ee*; 45% yield
(–)-2a: 87% *ee*; 44% yield

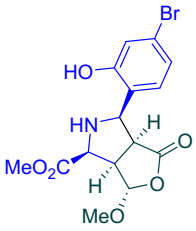

c = 41%; *s* = 80
4i: 95% *ee*; 40% yield
(–)-2a: 68% *ee*; 44% yield

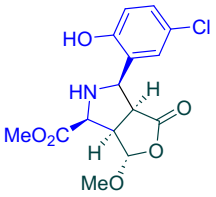

c = 37%; *s* = 49
4j: 93% *ee*; 35% yield
(–)-2a:56% *ee*; 39% yield

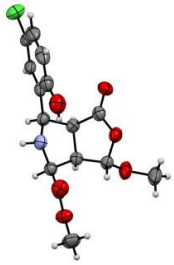

Aromatic substitution at aldimine: EWGs

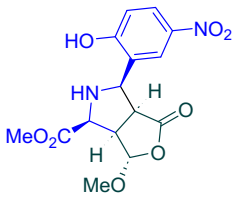

c = 49%; *s* = 120
4k: 95% *ee*; 47% yield
(–)-2a:90% *ee*; 40% yield

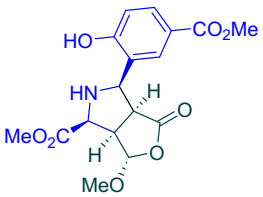

c = 38%; *s* = 37
4l: 91% *ee*; 35% yield
(–)-2a: 56% *ee*; 54% yield

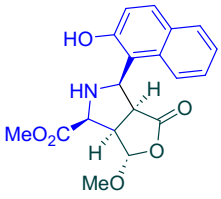

c[a] = 50%; *s* = 90
4m: 93% *ee*; 46% yield
(–)-2a: 91% *ee*; 45% yield

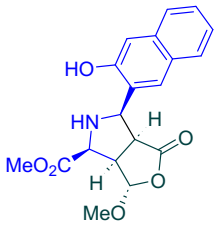

c[a] = 25%; *s* = 90
4n: 97% *ee*; 33% yield
(–)-2a: 33% *ee*; 49% yield

α-Substitution and EWG at aldimine

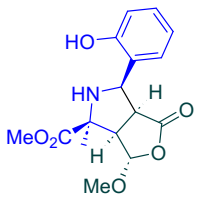

c = 51%; *s* = 45
4o: 87% *ee*; 46% yield
(–)-2a:91% *ee*; 47% yield

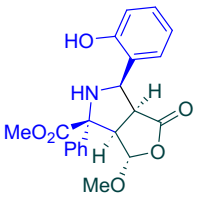

c = 48%; *s* = 11
4p:71% *ee*; 36% yield; 5:1 *dr*
(–)-2a: 65% *ee*; 48%

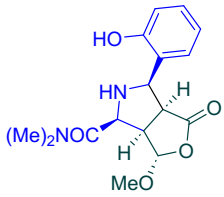

c = 49%; *s* = 29
4q: 84% *ee*; 44% yield
(–)-2a: 82% *ee*; 46% yield

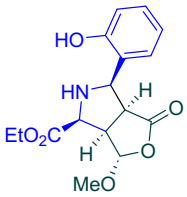

c = 48%; *s* = 80
4r: 93% *ee*; 47% yield
(–)-2a: 87% *ee*; 44% yield

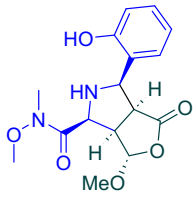

c = 52%; *s* = 100
4s: 90% *ee*; 48% yield
(–)-2a: 99% *ee*; 46% yield

Scheme 3. Scope of the [3+2] cycloaddition kinetic resolution. Reaction conditions: **1** (0.1 mmol), **(±)-2** (0.1 mmol), **3a** (20 mol%), *p*-xylene (0.3 mL), rt for 24h unless noted. Isolated yields shown. Enantiomeric ratio was measured by SFC. Calculated conversion (c)=$ee_{SM}/(ee_{SM}+ee_{PR})$. Selectivity factor (*s*)=ln[(1-c)(1-ee_{SM})]/ln[(1-c)(1+ee_{SM})]. [a] Reaction was carried out at 50 °C for 2 days.

View Article Online
DOI: 10.1039/D3QO01471A

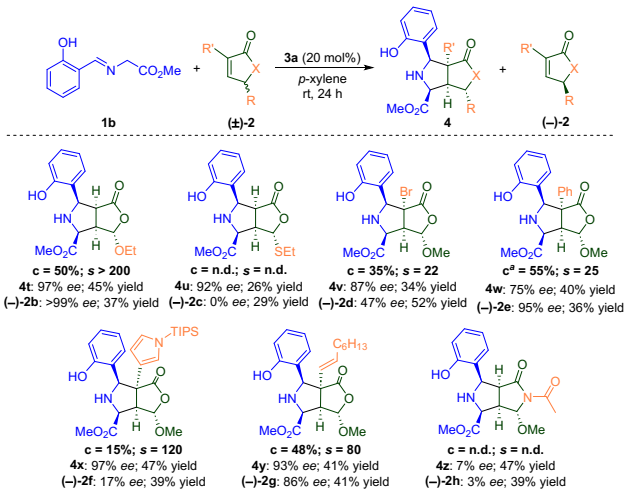

Scheme 4. Scope of the [3+2] cycloaddition kinetic resolution regarding to furanone and derivatives. Reaction conditions: **1** (0.1 mmol), **(±)-2** (0.1 mmol), **3a** (20 mol%), *p*-xylene (0.3 mL), rt for 24h unless noted. Isolated yields shown. Enantiomeric ratio was measured by SFC. Calculated conversion (c)=$ee_{SM}/(ee_{SM}+ee_{PR})$. Selectivity factor (*s*)=ln[(1-c)(1-ee_{SM})]/ln[(1-c)(1+ee_{SM})]. [a] Reaction was carried out at 0 °C in toluene.

Introducing a thiolate group resulted in the successful formation of the cycloadduct **4u** with a high degree of enantioselectivity (92% ee). However, the furanone **2c** was obtained with no enantioselectivity. This observation can be attributed to the high acidity of the thioacetal proton (H-5) in furanone **2c**, which can lead to complete epimerization in the presence of organocatalyst **3a**, resulting in a racemic mixture, followed by auto-selfcondensation as it was previously described in the literature.[24] The reaction with a more reactive *pseudo* ester as the 3-bromo-5-methoxyfuran-2(5*H*)-one (**(±)-2d**) was studied under the optimized conditions, achieving the cycloadduct **4v** with good enantioselectivity (87% *ee*) and moderate conversion (c = 35%) and selectivity. The reactions with aromatic derivative **(±)-2e** worked well, giving rise to cycloadducts **4w** with good selectivity, while heteroaromatic species **(±)-2f** gave the cycloadduct **4x** in excellent enantioselectivity (s = 120), but at low conversion, accounting for the recovery of the pyrrole derivative **(–)-2f** in low enantiomeric excess. With the incorporation of an alkenyl group the cycloaddition reaction is facile, leading to the formation of the corresponding adduct **4y** and the pseudoester (-)-**2g** with excellent enantioselectivities and yields. Notably, in these recent examples, it was possible to generate a quaternary carbon stereocenter in a precisely controlled manner. In contrast, we also studied the reactivity of 5-methoxypyrrol-2(5*H*)-ones containing an acetyl substituent at the nitrogen atom. Regrettably, under the specified conditions the acetyl derivative (±)-**2h** reacted to give the lactam **4z** and 2-(5*H*)-pyrrolone **2h** in high yield, but as a racemic mixture. Furthermore, attempts were made to conduct [3+2] cycloaddition reactions using 5-methoxyfuran-2(5*H*)-ones containing a methyl substituent at the alpha position. However, no conversion was observed in these reactions.

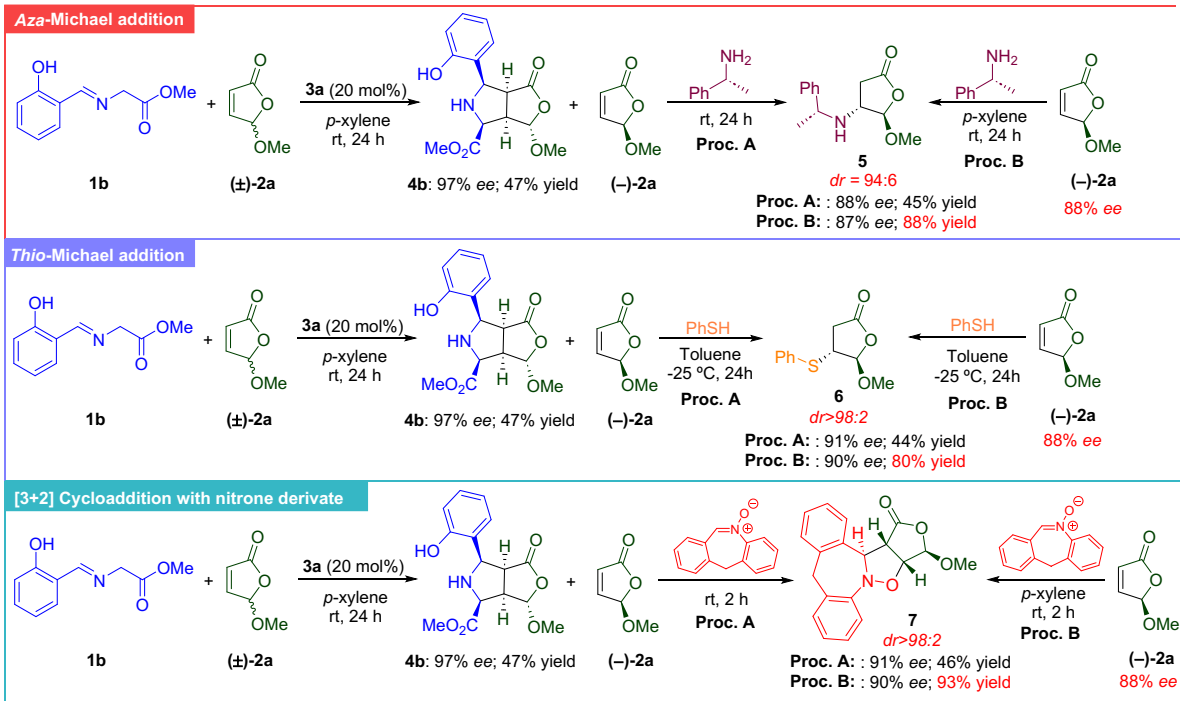

Scheme 5. Further derivatizations of **(–)-2a** in one pot and direct procedures. One-pot (**Proc. A**) and direct (**Proc. B**) procedures: [a] *Aza*-Michael addition of *(S)*-1-phenylethanamine to resolved **(–)-2a**. [b] *Thio*-Michael addition of thiophenol to resolved **(–)-2a**. [c] [3+2] cycloaddition of nitrone to resolved **(–)-2a**. Reactions were carried out at 0.1 mmol and 0.05 mmol scale for procedure A and B, respectively.

View Article Online
DOI: 10.1039/D3QO01471A

Considering the excellent results obtained in the kinetic resolution of 5-methoxyfuran-2(*5H*)-one (**(±)-2a**) and to showcase the utility of the developed process, we envisioned the use of the enantioenriched isomer **(–)-2a** as starting material for new asymmetric reactions (Scheme 5). Thus, the crude reaction product obtained during the [3+2] cycloaddition was submitted to a *one-pot* procedure. Therefore, several Michael additions[14g] and a [3+2] cycloaddition[18b] were carried out to demonstrate the applicability of our methodology (Proc. A, Scheme 5). Thus, the addition of (*R*)-1-phenylethan-1-amine or thiophenol to the crude reaction mixture from the cycloaddition (equations a and b) afforded the corresponding *aza*-Michael or *thio*-Michael products (**5** and **6**, respectively) with excellent enantio- and diastereo-selectivity and in high yields (only a 50% of final product can be obtained). Furthermore, the addition of 11*H*-dibenzo[*b*,*e*]azepine 5-oxide lead to the cycloadduct **7** with excellent results (equation c).

Finally, to corroborate the configurational stability of furanone, the same reactions showed before, starting from the cycloaddition reaction crudes, were conducted from the (*R*)-5-methoxyfuran-2(*5H*)-one (**(–)-2a**) obtained by the kinetic resolution and the subsequent purification by flash chromatography on silica gel (Proc. B, Scheme 5). The enantiomeric excesses achieved in these transformations brought to light that the 5-methoxyfuran-2(*5H*)-one (**(–)-2a**) obtained by kinetic resolution is configurationally stable and can be isolated in enantioenriched form without any racemization.

Mechanistic proposal

Once the scope of this organocatalyzed [3+2] asymmetric cycloaddition and the synthetic applicability of this kinetic resolution was demonstrated, we wished to rationalise the stereochemical outcome of this process. Taking into account the absolute configuration of final adducts **5**, an *endo* approach of ylide **1** in its *anti*-conformation, to the less hindered face of the furanone **2** (*anti-approach*), takes place. To corroborate this proposal, quantum chemistry calculations were carried out to obtain further theoretically insights on the enantioselectivity of the reaction.[25] We initially considered the possible relative orientations between catalyst **3a** and reactants **1b** and **(±)-2a**. Thus, we followed a similar strategy to that previously proposed,[26] which consist on a systematic exploration of the Potential Energy Surface (PES) using the GFN2-xTB method[27] as implemented in the CREST code.[28] From the most stable structures found with this method, the PES was refined using density functional theory (DFT), by combining the B3LYP functional and the 6-31+G(d,p) basis set, and including dispersion forces through the D3 version of Grimme's method with the Becke-Johnson damping.[29] These calculations were carried out with Gaussian16 code.[30]

The reaction was studied considering the *endo* approach for the two enantiomers of **2** (*exo* approaches were discarded since they are less favourable than *endo* ones,[15c,21b] see S.I.).[25] We considered a two-step process. The first step is the activation of the imine **1b** by an H transfer from **1b** to catalyst **3a**. In a second step, the new C-C bonds are formed, yielding the 5-membered ring (Figures 1 and 2, respectively). For both enantiomers, the H transfer requires ~18 kcal·mol^{-1} from the initial pre-association complex, PAC (pre-H transfer: complex formed by the catalyst and the two reactants **1b** and **(±)-2a**) (Figure 1).

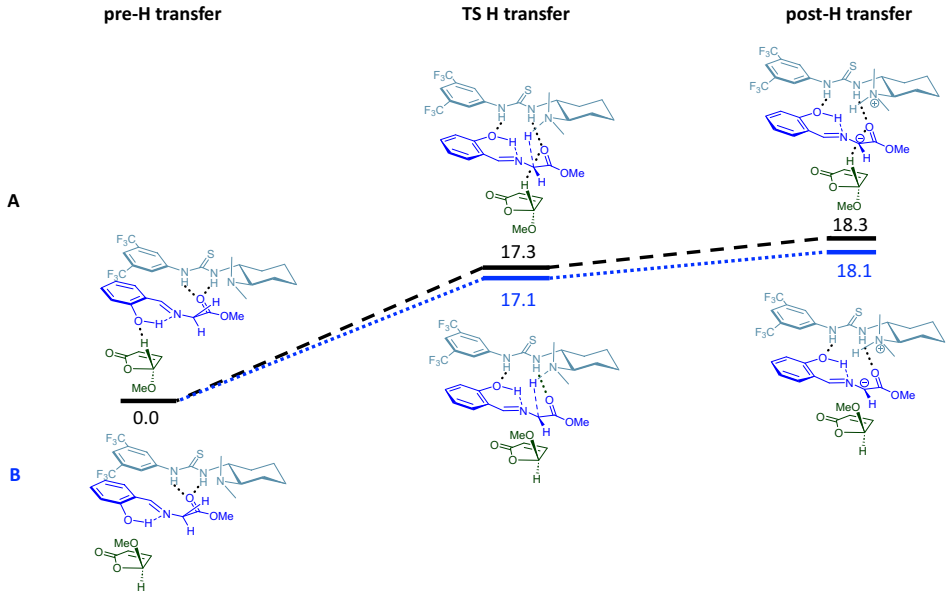

Figure 1. Potential energy surface for the H transfer reaction and the structures corresponding to the stationary states, both for the path leading to the observed product (**A**) and the path for the not observed enantiomer (**B**). Relative Gibbs free energies in kcal·mol^{-1} are referred to the pre-H transfer complex.

View Article Online
DOI: 10.1039/D3QO01471A

However, the main difference was found in the second cycloaddition step (Figure 2). While for the TS leading to the formed cycloadduct a low barrier of ~3.5 kcal·mol^{-1} is observed (black line), in the alternative case a transition state was located at much higher energy, ~9 kcal·mol^{-1} (blue line) with respect to the initial pre-association-complex (PAC, Figure 2); i.e., even higher than the first TS for H transfer. Therefore, for the non-observed isomer, the much higher barrier for the cycloaddition prevents its formation, thus explaining the experimentally obtained adduct.

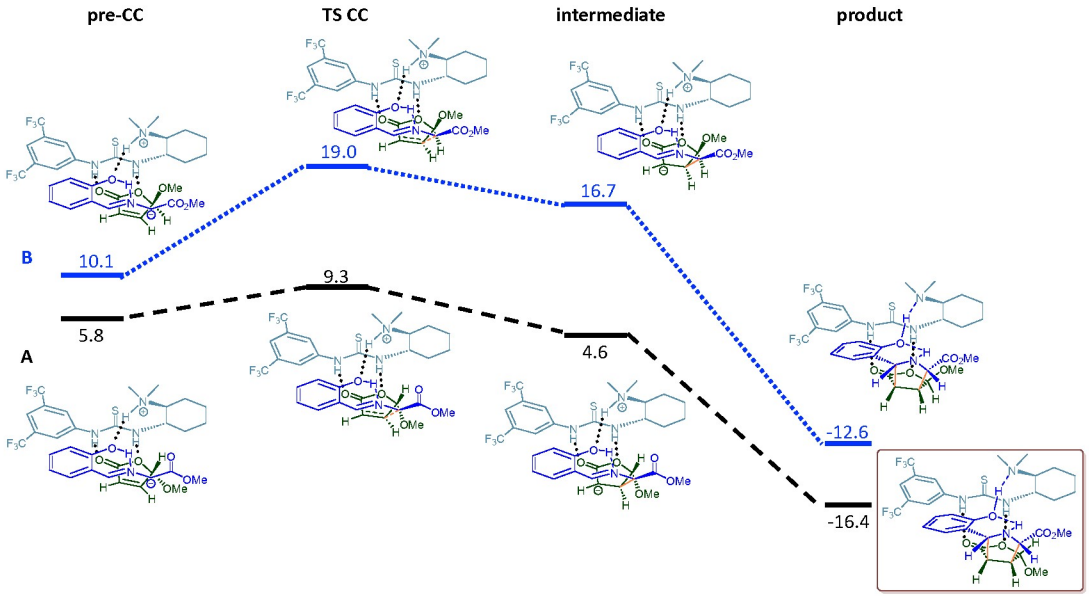

Figure 2. Potential energy surface for the CC bond formation and the structures corresponding to the stationary states, both for the path leading to the observed product (**A**, black line) and the path for the not observed enantiomer (**B**, blue line). Relative Gibbs free energies in kcal·mol^{-1} are referred to the pre-**H** transfer complex.

To provide further molecular insights on the origin of the stereocontrol, we analysed the non-covalent interaction (NCI) at the second TS (TS CC, Figure 3) by mean of NCI plots, using NCI code.[31] NCI plots show the different interaction regions using a colour code to rank those interactions. Red is used for destabilizing interactions, blue for stabilizing interactions and green for delocalized weak interactions. The intensity of these colours is associated with the interaction strength.

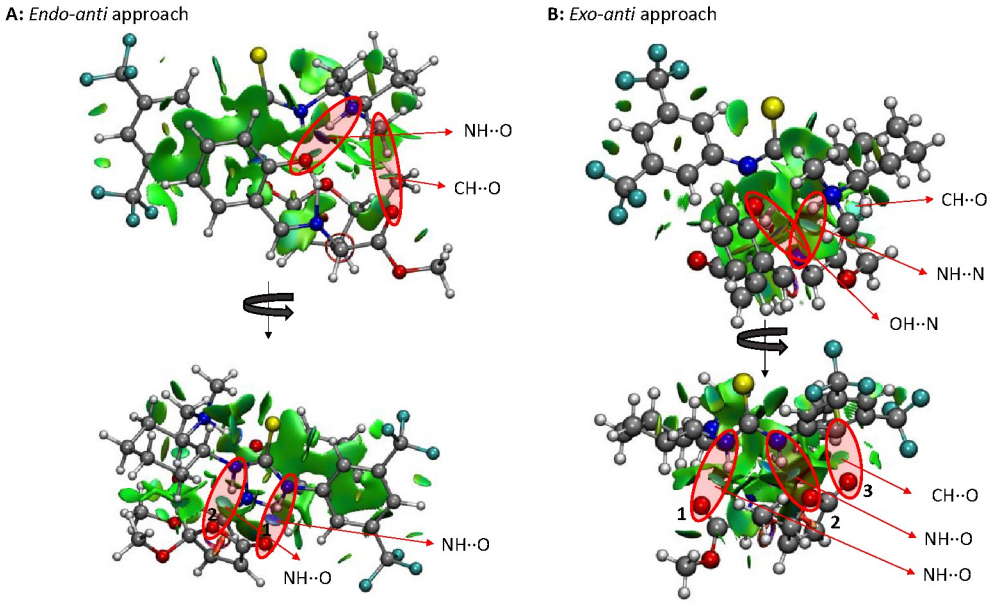

Figure 3. Noncovalent interaction (NCI) plot for the C-C bond formation transition states leading to the observed product (**A**) and the isomer (**B**). The green, blue, and red regions respectively represent attractive, strongly attractive, and repulsive interactions.

View Article Online
DOI: 10.1039/D3QO01471A

For both TS, NCI plots revealed weak delocalized interactions (green) between the three moieties interacting (Figure 3). However, the orientation of **1b** and both enantiomeric dipolarophiles **2a** with respect to the catalyst are slightly different, leading to different non-covalent interactions in the C-C bond forming transition state. TS-A (observed reaction) presents a strong NH··O hydrogen bond (blue flat circular region) between the ammonium group, generated after the H transfer to the catalyst and the hydroxy group of ylide **1b** (top image in Figure 3A). This leads to a stronger intramolecular hydrogen bond in **1b** between hydroxy group and the iminic nitrogen (actually it appears as H bonded to both atoms). While for TS-B, this hydrogen bond is formed with the iminic nitrogen of **1b** (instead of hydroxy group) and is weaker (only slightly blue) (top image in Figure 3B). The significance of the hydroxyl group on the aromatic ring of the imine becomes apparent from these findings. It plays a crucial role in establishing a beneficial intermolecular interaction with the organocatalyst through hydrogen bonding. In contrast, the absence of this hydroxyl group in imine **1a** prevents such an interaction, making it impossible to form a structured and organized complex between **1a** and **3a**. Consequently, this leads to low enantioselectivity.

Concerning the NCI between catalyst and dipolarophile **2a**, at TS-A there are two hydrogen bonds between the thiourea group at catalyst and oxygen atoms *1* and *2* at **( )-2a**, being *1* the stronger one (bottom image in Figure 3A). For TS-B (not-formed adduct), the different orientation of the methoxy group of **(–)-2a** allows the formation of a very weak hydrogen bond (green) between carbonyl oxygen atom *1* at the ylide **1b** (bottom image in Figure 3B) and the catalyst, displacing the furanone unit to the right.

This displacement provokes that only one hydrogen bond between oxygen *2* at furanone **(–)-2a** (NH··O) and the catalyst is formed being weaker than in TS-A (lighter blue color). In addition, for TS-B, there is a third CH··O bond (*3*), not present in TS-A, but it is very weak (green). The arrangement of the reactants at TS-B makes the region between the three moieties more crowded than in TS-A, hampering the approach of the two reactants to form the new C-C bond. This is reflected in a higher barrier for CC bond formation (TS-B energy is ~10 kcal·mol^{-1} higher than TS-A).

Conclusions

In conclusion, in this work we report an organocatalyzed [3+2] enantioselective cycloaddition of formal azomethine ylides with racemic furan-2(*5H*)-ones. This allows the generation of highly functionalized and versatile bicyclic adducts with up to 5 contiguous stereogenic centres in a stereocontrolled *endo* approach and with high enantioselectivities (up to 99% *ee*) due to the presence of the hydroxyl group at the aromatic ring of imines. Moreover, this cycloaddition reaction is paired to an efficient kinetic resolution of the furan-2(*5H*)-one, leading to the resolved substrate in enantioenriched form (up to 99% *ee*). This kinetic resolution takes place with selectivity factors up to 200 and very high conversions. DFT calculations have demonstrated the great effectiveness of the organocatalyzed [3+2] asymmetric cycloaddition to reach a very efficient kinetic resolution and the crucial influence of the hydroxyl group at the imine aromatic ring on the deprotonation process to generate the reactive ylide and on the stereoselectivity.

Data availability

Experimental details, general procedures, optimization of reaction conditions, characterization of products, copies of NMR and HPLC spectra of all products and computational details are in the ESI.

Author Contributions

A. F. and J. A. conceived, designed, and supervised this work. M. A. V.-A. and C. F. performed the experiments and the synthesis and characterizations of new compounds. A. F. and M. A. V.-A prepared the ESI. A. F., J. A., M. A. V.-A and A. D. S. wrote the article. All authors contributed to the discussion of the results.

Conflicts of interest

There are no conflicts to declare.

Acknowledgements

This work was supported by Spanish Ministry of Science and Innovation (projects PID2019-110091GB-I00, PID2021-122299NB-I00, TED2021-130470B-I00, TED2021-129999B-C32), "Comunidad de Madrid" for European Structural Funds (S2018/NMT-4367) and proyectos sinérgicos I+D (Y2020/NMT-6469), and the "María de Maeztu" (CEX2018-000805-M) Program for Centers of Excellence in R&D. A.M.S. thanks the Madrid Government (Comunidad de Madrid-Spain) under the Multiannual Agreement with Universidad Autónoma de Madrid in the line Support to Young Researchers, in the context of the V PRICIT (SI3-PJI-2021-00463). C. F. thanks Ministerio de Universidades for a Margarita Salas grant. In addition, authors acknowledge the generous allocation of computer time at the Centro de Computación Científica at the Universidad Autónoma de Madrid (CCC-UAM).

Notes and references

1 (*a*) H. B. Kagan and J. C. Fiaud, In *Topic in Stereochemistry*, Vol. 18; E. L. Eliel and S. H. Wilen, Eds.; John Wiley & Sons, Inc.; **1988**, Ch 4, pp 249–330; (*b*) *Enantiomers, Racemates, and Resolutions*; J. Jacques, A. Collet and S. H. Wilen, Eds.; John Wiley & Sons, Inc.; **1981**; (*c*) *Separation of Enantiomers: Synthetic Methods*; M. H. Todd, Eds.; Wiley-VCH; Weinheim, Germany **2014**.

2 (*a*) X.-C. He and C.-Y. Qi, Practical Tactics in Resolution of Racemates via Diastereomeric Salt Formation, *Chin. J. Chem.*, 2007*,* **25**, 583–586; (*b*) M. R. Maddani, J.-C. Fiaud and H. B.

View Article Online
DOI: 10.1039/D3QO01471A

Kagan, Stoichiometric Kinetic Resolution Reactions. In *Separation of Enantiomers: Synthetic Methods*; M. H. Todd, Eds.; Wiley-VCH; Weinheim, Germany **2014**, Ch 2, pp 13–74; (*c*) S.-Y. Hsieh, B. Wanner, P. Wheeler, A. M. Beauchemin, T. Rovis and J. W. Bode, Stereoelectronic Basis for the Kinetic Resolution of *N*-Heterocycles with Chiral Acylating Reagents, *Chem. Eur. J.*, 2014, **20**, 7228–7231.

3 (*a*) H. Pellissier, Catalytic Kinetic Resolution. In *Separation of Enantiomers: Synthetic Methods*; M. H. Todd, Eds.; Wiley-VCH; Weinheim, Germany **2014**, Ch 3, pp 75–122; (*b*) E. R. Jarvo and S. J. Miller, Acylation Reaction. In *Comprehensive Asymmetric Catalysis*, Supplement 1; E. N. Jacobsen, A. Pfaltz, H. Yamamoto, Eds.; Springer-Verlag Berlin, Heidelberg **2004**, Ch 43, pp 189–206; (*c*) J. M. Keith, J. F. Larrow and E. N Jacobsen, Practical Considerations in Kinetic Resolution Reactions, *Adv. Synth. Catal.*, 2001, **343**, 5–26.

4 M. D. Greenhalgh, J. E. Taylor and A. D. Smith, Best Practice Considerations for Using the Selectivity Factor, *s*, as a Metric for the Efficiency of Kinetic Resolutions, *Tetrahedron*, 2018, **74**, 5554–5560.

5 (*a*) A. Ghanem and H. Y. Aboul-Enein, Application of Lipases in Kinetic Resolution of Racemates, *Chirality*, 2005, **17**, 1–15; (*b*) M. T. Reetz, Biocatalysis in Organic Chemistry and Biotechnology: Past, Present, and Future, *J. Am. Chem. Soc.*, 2013, **135**, 12480–12496; (*c*) C. E. Humphrey, M. Ahmed, A. Ghanem and N. J. Turnerx, Application of Enzymes in Kinetic Resolutions, Dynamic Kinetic Resolutions and Deracemization Reactions. In *Separation of Enantiomers: Synthetic Methods*; M. H. Todd, Eds.; Wiley-VCH; Weinheim, Germany **2014**, Ch 4, pp 123–160; (*d*) S. Wu, R. Snajdrova, J. C. Moore, K. Baldenius and U. T. Bornscheuer, Biocatalysis: Enzymatic Synthesis for Industrial Applications, *Angew. Chem. Int. Ed.*, 2021, **60**, 88–119; (*e*) Q. H. Zhang, Y. Fang, W. F. Luo and L. N. Huang, Biocatalytic Kinetic Resolution of D,L-pantolactone by Using a Novel Recombinant D-Lactonase, *RSC Advances*, 2021, **11**, 721–725; (*f*) Q. H. Zhang, L. Yang, Y. B. Tang, L. N. Huang and W. F. Luo, Industrial Kinetic Resolution of D,L-Pantolactone by an Immobilized Whole-Cell Biocatalyst, *RSC Advances*, 2021, **11**, 30373–30376.

6 (*a*) D. E. J. E. Robinson and S. D. Bull, Kinetic Resolution Strategies Using Non-Enzymatic Catalysts, *Tetrahedron: Asymmetry*, 2003, **14**, 1407–1446; (*b*) E. Vedejs and M. Jure, Efficiency in Nonenzymatic Kinetic Resolution, *Angew. Chem. Int. Ed.*, 2005, **44**, 3974–4001; (*c*) H. Pellissier, Catalytic Non-Enzymatic Kinetic Resolution, *Adv. Synth. Catal.*, 2011, **353**, 1613–1666.

7 (*a*) A. H. Hoveyda and M. T. Didiuk, Metal-Catalyzed Kinetic Resolution Processes, *Curr. Org. Chem.*, 1998, **2**, 489–526; (*b*) G. R. Cook, Transition Metal-Mediated Kinetic Resolution, *Curr. Org. Chem.*, 2000, **4**, 869–885; (*c*) L. Deng, Y. Fu, S. Y. Lee, C. Wang, P. Liu and G. Dong, Kinetic Resolution via Rh-Catalyzed C–C Activation of Cyclobutanones at Room Temperature, *J. Am. Chem. Soc.*, 2019, **141**, 16260–16265; (*d*) J. M. González, B. Cendón, J. L. Mascareñas and M. Gulías, Kinetic Resolution of Allyltriflamides through a Pd-Catalyzed C–H Functionalization with Allenes: Asymmetric Assembly of Tetrahydropyridines, *J. Am. Chem. Soc.*, 2021, **143**, 3747–3752.

8 (*a*) R. Gurubrahamam, Y.-S. Cheng, W.-Y. Huang and K. Chen, Recent Advances in Organocatalytic Kinetic Resolution for the Synthesis of Functionalized Products, *ChemCatChem*, 2016, **8**, 86–96 and references therein cited; (*b*) U. Farid, M. L. Aiello and S. J. Connon, Highly Enantioselective Catalytic Kinetic Resolution of α-Branch, d Aldehydes through Formal Cycloaddition with Homophthalic Anhydrides, *Chem. Eur. J.*, 2019, **25**, 10074–10079; (*c*) S. Qu, S. M. Smith, V. Laina-Martín, R. M. Neyyappadath, M. D. Greenhalgh and A. D. Smith, Isothiourea-Catalyzed Acylative Kinetic Resolution of Tertiary α-Hydroxy Esters, *Angew. Chem. Int. Ed.*, 2020, **59**, 16572–16578; (*d*) J. Liu, L. Vasamsetty, M. Anwar, S. Yang, W. Xu, J. Liu, S. Nagaraju and X. Fang, Organocatalyzed Kinetic Resolution of α-Functionalized Ketones: The Malonate Unit Leads the Way, *ACS Catal.*, 2020, **10**, 2882–2893; (*e*) S. Sun, Z. Wang, S. Li, C. Zhou, L. Song, H. Huang, and J. Sun, An Organocatalytic Kinetic Resolution of Aziridines by Thiol Nucleophiles, *Org. Lett.*, 2021, **23**, 554–558; (*f*) Y. Wu, M. Li, J. Sun, G. Zheng and Q. Zhang, Synthesis of Axially Chiral Aldehydes by N-Heterocyclic-Carbene-Catalyzed Desymmetrization Followed by Kinetic Resolution, *Angew. Chem. Int. Ed.*, 2022, **61**, e202117340; (*g*) S. Barik, R. C. Das, K. Balanna and A. T. Biju, Kinetic Resolution Approach to the Synthesis of C–N Axially Chiral N-Aryl Aminomaleimides via NHC-Catalyzed [3 + 3] Annulation, *Org. Lett.*, 2022, **24**, 5456–5461.

9 A. Suárez, C. W. Downey and G. C. Fu, Kinetic Resolutions of Azomethine Imines via Copper-Catalyzed [3 + 2] Cycloadditions, *J. Am. Chem. Soc.*, 2005, **127**, 11244–11245.

10 (*a*) H. Takayama, Z.-J. Jia, L. Kremer, J. O. Bauer, C. Strohmann, S. Ziegler, A. P. Antonchick and H. Waldmann, Discovery of Inhibitors of the Wnt and Hedgehog Signaling Pathways through the Catalytic Enantioselective Synthesis of an Iridoid-Inspired Compound Collection, *Angew. Chem. Int. Ed.*, 2013, **52**, 12404–12408; (*b*) H. Xu, C. Golz, C. Strohmann, A. P. Antonchick and H. Waldmann, Enantiodivergent Combination of Natural Product Scaffolds Enabled by Catalytic Enantioselective Cycloaddition, *Angew. Chem. Int. Ed.*, 2016, **55**, 7761–7765; (*c*) Y. Yuan, Z.-J. Zheng, L. Li, X.-F. Bai, Z. Xu, Y.-M. Cui, J. Cao, K.-F. Yang and L.-W. Xu, Silicon-based Bulky Group−Tun, d Parallel Kinetic Resolution in Copper-Catalyzed 1,3-Dipolar Additions, *Adv. Synth. Catal.*, 2018, **360**, 3002–3008; (*d*) C. Shen, Y. Yang, L. Wei, W.-W. Dong, L. W. Chung and C.-J. Wang, Kinetic Resolution of Alkylidene Norcamphors via a Ligand-Controlled Umpolung-Type 1,3-Dipolar Cycloaddition, *iScience*, 2019, **11**, 146–159; (*e*) H. Deng, T.-T. Liu, Z.-D. Ding, W.-L. Yang, X. Luo and W.-P. Deng, Kinetic resolution of 2H-azirines via Cu(I)-catalyzed asymmetric 1,3-dipolar cycloaddition of azomethine ylides, *Org. Chem. Front.*, 2020, **7**, 3247–3252.

11 J.-W. Xie, L.-P. Fan, H. Su, X.-S. Li and D.-C. Xu, Efficient kinetic resolution of racemic 3-nitro-2H-chromene derivatives catalyzed by Takemoto's organocatalyst, *Org. Biomol. Chem.*, 2010, **8**, 2117–2122.

12 J. Yu, W.-J. Chen and L.-Z. Gong, Kinetic Resolution of Racemic 2,3-Allenoates by Organocatalytic Asymmetric 1,3-Dipolar Cycloaddition, *Org. Lett.*, 2010, **12**, 4050–4053.

13 A. Husain, S. A. Khan, F. Iram, M. A. Iqbal and M. Asif, Insights into the chemistry and therapeutic potential of furanones: A versatile pharmacophore, *Eur. J. Med. Chem.*, 2019, **171**, 66–92 and references cited therein.

14 (*a*) F. Fariña, M. V. Martín and F. Sánchez, Pseudoesters and Derivatives. XXIV. 1,3-Dipolar Cycloaddition of Diazomethane to 5-Methoxyfuran-2(5*H*)-ones, *Heterocycles*, 1986, **24**, 2587–2592; (*b*) L. Fišera and P. Oravec, Stereoselectivity of Cycloadditions of Arylnitrile Oxides to 5-Alkoxy-2(5*H*)-furanone, *Collect. Czech. Chem. Commun.*, 1987, **52**, 1315–1324; (*c*) B. L. Feringa and B. de Lange, Asymmetric 1,4-Additions to 5-Alkoxy-2(5*H*)-furanones: An Efficient Synthesis of (*R*)- and (*S*)-3,4-Epoxy-1-Butanol, *Tetrahedron*, 1988, **44**, 7213–7222; (*d*) B. L. Feringa and B. de Lange, 1,4-Additions of Amines to 5-Methoxyfuran-2(5*H*)-one; an Efficient Synthesis of Amino Diols, *Heterocycles*, 1988, **27**, 1197–1205; (*e*) E. Keller, B. de Lange, M. T. Rispens and B. L. Feringa, 1,3-Dipolar Cycloadditions to 5-Methoxy-2(5*H*)-furanone, *Tetrahedron*, 1993, **49**, 8899–8910; (*f*) F. Fariña, M. R. Martín, M. V. Martín and A. Martinez de Guereñu, Cycloaddition of Nitrile Oxides to 4-Oxobut-2-enoic Acid

View Article Online
DOI: 10.1039/D3QO01471A

Derivatives, *Heterocycles*, 1994, **38**, 1307–1316; (*g*) W. S. Faber, J. Kok, B. de Lange and B. L. Feringa, Catalytic Kinetic Resolution of 5-Alkoxy-2(5*H*)-furanones, *Tetrahedron*, 1994, **50**, 4775–4794.

15 (a) J. L. García Ruano, A. Fraile, M. R. Martín and A. Núñez, First Asymmetric Cycloaddition of Carbonyl Ylides to Vinyl Sulfoxides and Furan-2(5*H*)-ones, *J. Org. Chem.*, 2006, **71**, 6536–6541; (*b*) A. Núñez Jr., M. R. Martín, A. Fraile and J. L. García Ruano, Abnormal Behaviour of Allenylsulfones under Lu's Reaction Conditions: Synthesis of Enantiopure Polyfunctionalised Cyclopentenes, *Chem. Eur. J.*, 2010, **16**, 5443–5453; (*c*) J. L. García Ruano, A. Fraile, M. R. Martín, G. González, C. Fajardo and A. M. Martín-Castro, Asymmetric Synthesis of Pyrrolo[2,1-*a*]isoquinoline Derivatives by 1,3-Dipolar Cycloadditions of Stabilized Isoquinolinium *N*-Ylides with Sulfinyl Dipolarophiles, *J. Org. Chem.*, 2011, **76**, 3296–3305.

16 (*a*) B. L. Feringa and J. C. de Jong, New Strategies in Asymmetric Synthesis Based on γ-Alkoxybutenoljd, *Bull. Soc. Chim. Belg.*, 1992, **101**, 627–640; (*b*) B. L. Feringa, B. de Lange, J. F. G. A. Jansen, J. C. de Jong, M. Lubben, W. Faber and E. P. Schudde, New Approaches in Asymmetric Synthesis Using γ-Alkoxybutenoljd, *Pure & Appl. Chem*., 1992, **64**, 1865–1871 and therein references cited.

17 (*a*) D. M. Cooper, R. Grigg, S. Hargreaves, P. Kennewell and J. Redpath, X=Y-ZH Compounds as Potential 1,3-Dipoles. Part 44.[1] Asymmetric 1,3-Dipolar Cycloaddition Reactions of Imines and Chiral Cyclic Dipolarophiles, *Tetrahedron*, 1995, **51**, 7791–7808; (*b*) H. A. Dondas, R. Grigg and M. Thornton-Pett, Spiro(, yrroljdiny,-2,3'-Benzodiazepines) Related to MK-329, *Tetrahedron*, 1996, **52**, 13455–13466; (*c*) B. M. Trost and M. L. Crawley, A "Chiral Aldehyde" Equivalent as a Building Block Towards Biologically Active Targets, *Chem. Eur. J.*, 2004, **10**, 2237–2252; (*d*) R. Grigg, D. M. Cooper, S. Holloway, S. McDonald, E. Millingtona and M. A. B. Sarker, X=Y–ZH Systems as Potential 1,3-Dipoles. Part 61: Metal Exchanged Zeolites, Silver(I) Oxide, Ni(II) and Cu(I) Complexes as Catalysts for 1,3-Dipolar Cycloaddition Reactions of Imines Generating Proline Derivatives, *Tetrahedron*, 2005, **61**, 8677–8685.

18 (*a*) J. L. García Ruano, A. Fraile and M. R. Martín, (*Ss*)-5-Ethoxy-3-*p*-Tolylsulfinylfuran-2(5*H*)-ones as Chiral Dipolarophiles: First Asymmetric Cycloaddition of Diazomethane to Vinyl Sulfoxides, *Tetrahedron Asymmetric*, 1996, **7**, 1943–1950; (*b*) J. L. García Ruano, J. I. Andrés Gil, A. Fraile, A. M. Martín Castro and M. R. Martín, Asymmetric 1,3-Dipolar Reactions of 3-Sulfinylfuran-2(5*H*)-ones with 11*H*-Dibenzo[*b,e*]azepine 5-Oxide. Synthesis of Pyrroloazepines via Isoxazoloazepines, *Tetrahedron Lett.*, 2004, **45**, 4653–4656; (*c*) J. L. García Ruano, A. Fraile, A. M. Martín Castro and M. R. Martín, The Role of the Sulfinyl Group on the Course of the Reactions of 3-*p*-Tolylsulfinylfuran-2(5*H*)-ones with Nitrones. Synthetic Uses of Cycloreversion Processes, *J. Org. Chem.*, 2005, **70**, 8825–8834; (*d*) J. L. García Ruano, A. Núñez Jr., M. R. Martín and A. Fraile, Totally Regio- and Stereoselective Behavior of Mono- and Diactivated Cyclic Alkenes in the Lu Reaction: Synthesis of Enantiopure Functionalized Cyclopentanes, *J. Org. Chem.*, 2008, **73**, 9366–9371.

19 *Green Chemistry: Theory and Practice*. P. T. Anastas and J. C. Warner, Eds; Oxford University Press, **1998**.

20 D. G. Blackmond, Kinetic Resolution Using Enantioimpure Catalγ,ts: Mechanistic Considerations of Complex Rate Laws, *J. Am. Chem. Soc.*, **2001**, *123*, 545–553.

21 (*a*) A. Guerrero-Corrella, M. A. Valle-Amores, A. Fraile and J. Alemán, Enantioselective Organocatalyzed *aza*-Michael Addition Reaction of 2-Hydroxybenzophenone Imines to Nitroolefins under Batch and Flow Conditions, *Adv. Synth. Catal.*, 2021, **363**, 3845–3851; (*b*) F. Esteban, W. Cieslik, E. M. Arpa, A. Guerrero-Corella, S. Díaz-Tendero, J. Perles, J. A. Fernández-Salas, A. Fraile, and J. Alemán, Intramolecular Hydrogen Bond Activation: Thiourea-Organocatalyzed Enantioselective 1,3-Dipolar Cycloaddition of Salicylaldehyde-Derived Azomethine Ylides with Nitroalkenes. *ACS Catal.*, 2018, **8**, 1884–1890; (*c*) A. Guerrero-Corella, A. Fraile and J. Alemán, Intramolecular Hydrogen-Bond Activation: Strategies, Benefits, and Influence in Catalysis, *ACS Org. Inorg. Au.*, 2022, **2**, 197–204.

22 A. Guerrero-Corella, F. Esteban, M. Iniesta, A. Martín-Somer, M. Parra, S. Díaz-Tendero, A. Fraile, and J. Alemán, 2-Hydroxybenzophenone as a Chemical Auxiliary for the Activation of Ketiminoesters for Highly Enantioselective Addition to Nitroalkenes under Bifunctional Catalysis, *Angew. Chem. Int. Ed.*, 2018, **57**, 5350–5354.

23 CCDC-2160961 (**4i**) contains the supplementary crystallographic data for this paper. These data can be obtained free of charge from The Cambridge Crystallographic Data Centre via www.ccdc.cam.ac.uk/data_request/cif.

24 F. Fariña and M. D. Parellada, Pseudoesters and Derivatives. 29. Regioselective Reactions of the 5-(Ethylthio)furan-2(5*H*)-one Anion with Electrophiles, *J. Org. Chem.*, 1988, **53**, 3330–3333.

25 (*a*) All the optimized structures computed can be visualized and download from http://dx.doi.org/10.19061/iochem-bd-8-10; (*b*) M. Álvarez-Moreno, C. de Graaf, N. Lopez, F. Maseras, J. M. Poblet and C. Bo, Managing the Computational Chemistry Big Data Problem: The ioChem-BD Platform, *J. Chem. Inf. Model.*, 2015, **55**, 95–103.

26 I. Iribarren and C. Trujillo, Efficiency and Suitability when Exploring the Conformational Space of Phase-Transfer Catalysts, *J. Chem. Inf. Model.*, 2022, **62**, 5568–5580.

27 C. Bannwarth, S. Ehlert and S. Grimme, GFN2-xTB–An Accurate and Broadly Parametrized Self-Consistent Tight-Binding Quantum Chemical Method with Multipole Electrostatics and Density-Dependent Dispersion Contributions, *J. Chem. Theory Comput.*, 2019, **15**, 1652–1671.

28 P. Pracht, F. Bohle and S. Grimme, Automated Exploration of the Low-Energy Chemical Space with Fast Quantum Chemical Methods, *Phys. Chem. Chem. Phys.*, 2020, **22**, 7169–7192.

29 S. Grimme, S. Ehrlich and L. Goerigk, Effect of the Damping Function in Dispersion Corrected Density Functional Theory, *J. Comp. Chem.*, 2011, **32**, 1456–1465.

30 M. J. Frisch et al., Gaussian 16, Revision C.01, Gaussian, Inc., Wallingford CT, **2019**.

31 (*a*) E. R. Johnson, S. Keinan, P. Mori-Sanchez, J. Contreras-García, A. J. Cohen and W. Yang, Revealing Noncovalent Interactions, *J. Am. Chem. Soc.*, 2010, **132**, 6498–6506; (*b*) J. Contreras-García, E. R. Johnson, S. Keinan, R. Chaudret, J.-P. Piquemal, D. N. Beratan and W. Yang, NCIPLOT: A Program for Plotting Non-Covalent Interaction Regions, *J. Chem. Theory Comput.*, 2011, **7**, 625–632.